THE JOURNAL OF NAVIGATION (2018), **71**, 134–150. © The Royal Institute of Navigation 2017
doi:10.1017/S0373463317000522

Integrated GNSS Attitude and Position Determination based on an Affine Constrained Model

Haiying Liu[1,2], Lei Xu[1], Xiaolin Meng[2], Xibei Chen[1] and Junyi Li[3]

[1](*College of Astronautics, Nanjing University of Aeronautics and Astronautics, Nanjing 210016, P. R. China*)
[2](*Nottingham Geospatial Institute and Sino-UK Geospatial Engineering Centre, University of Nottingham, Nottingham, NG7 2TU, UK*)
[3](*First Geodetic Team, National Administration of Surveying, Mapping and Geoinformation, Xi'an, China*)
(E-mail: liuhaiying@nuaa.edu.cn)

Global Navigation Satellite System (GNSS) attitude determination and positioning play an important role in many navigation applications. However, the two GNSS-based problems are usually treated separately. This ignores the constraint information of the GNSS antenna array and the accuracy is limited. To improve the performance of navigation, an integrated attitude and position determination method based on an affine constraint model is presented. In the first part, the GNSS array model and affine constrained attitude determination method are compared with the unconstrained methods. Then the integrated attitude and position determination method is presented. The performance of the proposed method is tested with a series of static data and dynamic experimental GNSS data. The results show that the proposed method can improve the success rate of ambiguity resolution to further improve the accuracy of attitude determination and relative positioning compared to the unconstrained methods.

KEYWORDS

1. GNSS. 2. Affine constraint.
3. Attitude determination. 4. Positioning.

Submitted: 2 January 2016. Accepted: 3 July 2017. First published online: 1 August 2017.

1. INTRODUCTION. In the field of navigation, guidance and control, the development of high performance Global Navigation Satellite System (GNSS) attitude determination and positioning are important. As GNSS has several advantages compared with other sensors, such as lower power consumption, lower maintenance and lower cost compared with other high-precision systems, it has been widely researched in recent years. Applications include, for instance, aircraft carrier landing (Li et al., 2013), airborne refuelling aircraft (Lee et al., 2014), satellite formation flying (Giorgi et al., 2011a; Yang et al., 2014) and

https://doi.org/10.1017/S0373463317000522 Published online by Cambridge University Press

intelligent transportation systems (Stephenson et al., 2014). Based on the GNSS carrier phase measurement, centimetre-level or even-millimetre level position accuracy can be obtained. In addition, multiple GNSS antennae mounted on a moving platform can provide independent attitude information.

Currently, most of the studies on GNSS attitude determination and positioning are carried out separately, that is, the positioning and orientation systems are designed independently. For example, in view of the positioning requirement, the Differential GNSS (DGNSS) and Real Time Kinematic (RTK) positioning methods have been developed using a carrier phase difference technique (Ardaens and Florio 2013). For attitude determination, different methods using GNSS multi-antenna systems are presented, such as the direct attitude computation method and the carrier smoothed pseudorange method (Dai et al., 2009; Baroni and Kuga, 2012; Nadarajah et al., 2014b). However, this approach does not take into account the baseline constraint of multi-antenna systems and the constrained information of relative multiple platforms, which limits the improvement of navigation accuracy. Meanwhile, in harsh environments (such as lacking visible satellites and multipath effects) the success rate of the position and attitude solution are further reduced.

High precision GNSS determination of attitude and positioning requires carrier phase ambiguity resolution. Over the last two decades considerable research on ambiguity resolution has been conducted, such as the Fast Ambiguity Resolution Approach (FARA) (Hofmann et al., 2008), Three/Multiple Carrier Ambiguity Resolution (TCAR/MCAR) (Werner and Winkel, 2003) and Least squares AMBiguity Decorrelation Adjustment (LAMBDA) (Teunissen, 2003; Teunissen and Verhagen, 2011). The fast integer least-squares estimation for high-dimensional ambiguity resolution using lattice theory was proposed (Jazaeri et al., 2014), and four well-known decorrelation algorithms, namely Lenstra-Lenstra-Lova'sz (LLL) (Lenstra et al., 1982), LAMBDA, Modified LAMBDA (MLAMBDA) (Seysen, 1993) have been compared, which indicated that LAMBDA and MLAMBDA perform much better in reducing the number of integer candidates than the other two algorithms.

The traditional attitude determination method did not effectively use the advantages of baseline information and multi-antenna constraint, which is referred to as the Unconstrained Attitude Model (UC-AM) (Giorgi et al., 2011a). A rigorous GNSS attitude model referred to as the Orthonormality Constrained Attitude Model (OC-AM) was proposed (Teunissen, 2007), which includes the whole set of nonlinear geometrical constraints of the antenna coordinates and the attitude matrix orthonormality constraint. Based on OC-AM, the Multivariate Constrained LAMBDA (MC-LAMBDA) was used for attitude ambiguity resolution (Giorgi et al., 2011b), and a step-by-step position and attitude determination method was proposed (Buist, 2013). A novel integrated attitude and position system was further studied to provide estimates for a Three-Dimensional (3D) laser scanner, which uses the MC-LAMBDA method for the estimation of rotating frame ambiguities and attitude angles (Nadarajah et al., 2014a).

Recently, a new Affine Constrained Attitude Model (AC-AM) was proposed for ambiguity resolution and attitude determination (Teunissen, 2012; Giorgi and Teunissen, 2013), with the advantage that it avoids the complexity of OC-AM and has a significantly improved performance over its UC-AM counterpart. In this paper, the AC-AM model is further studied and applied to integrated attitude position determination. A bootstrapping idea is adopted for an integrated system in this paper, which is similar to Nadarajah et al.

https://doi.org/10.1017/S0373463317000522 Published online by Cambridge University Press

(2014a) and Buist (2013). The first of these two references is based on the OC-AM and the second is studied for the unconstrained baseline. However, the AC-AM method has not yet been studied for an integrated system. Therefore, the main contribution of this paper is to apply the new AC-AM model to integrated attitude and position determination, and different static and dynamic test scenarios are designed to validate the proposed method.

This contribution is organised as follows: Section 2 describes the GNSS double-difference and array antenna model. Section 3 describes our integrated attitude and position approach using the AC-AM method. Section 4 presents a comparative analysis of our new method and the UC-AM methods using real GNSS static and dynamic experiment data. Finally, Section 5 contains the summary and conclusions of this contribution.

2. GNSS DOUBLE-DIFFERENCE AND ARRAY MODEL.

2.1. *GNSS Double-difference model.* For most GNSS attitude determination and positioning systems, the Double Difference (DD) technique between receivers and satellites is chosen since it can balance processing complexity, practicality and performance for real time implementation. By taking differences between two GNSS satellites (p, s) and two receivers (r, m) on frequency j, the DD code and carrier phase equations can be written as (Hofmann et al., 2008)

$$P^{ps}_{rm,j} = \rho^{ps}_{rm} + \mu_j I^{ps}_{rm} + T^{ps}_{rm} + e^{ps}_{rm} \tag{1}$$

$$\lambda_j \phi^{ps}_{rm,j} = \rho^{ps}_{rm} - \mu_j I^{ps}_{rm} + T^{ps}_{rm} - \lambda_j N^{ps}_{rm,j} + \varepsilon^{ps}_{rm} \tag{2}$$

where $P^{ps}_{rm,j} = \left(P^{p}_{r,j} - P^{s}_{r,j}\right) - \left(P^{p}_{m,j} - P^{p}_{m,j}\right)$ is the code DD on frequency j, and $\phi^{ps}_{rm,j} = \left(\phi^{p}_{r,j} - \phi^{s}_{r,j}\right) - \left(\phi^{p}_{m,j} - \phi^{s}_{m,j}\right)$ represents the carrier phase DD. The symbol ρ^{ps}_{rm} represents the combination of geometric distances between receivers and satellites, I^{ps}_{rm} represents the ionosphere delay with coefficient $\mu_j = \left(\lambda_j / \lambda_1\right)^2$, λ_j and λ_1 are the wavelength for the frequency j and the frequency of the first reference in DD equations. T^{ps}_{rm} represents the troposphere delay, $N^{ps}_{rm,j}$ is the DD ambiguity, and e^{ps}_{rm} and ε^{ps}_{rm} are error terms.

Equations (1) and (2) are the foundation for GNSS positioning and navigation.

2.2. *GNSS Array model.* Consider a platform equipped with $r+1$ GNSS antennae, as shown in Figure 1. The attitude of a platform is described by the orientation of its Antenna Body Frame (ABF) with respect to the reference frame Local Level Frame (LLF). Let the baseline vector from master antenna to slave antenna r in ABF be defined as $\boldsymbol{b}_i$ $(i = 1, 2, \ldots, r)$, and the corresponding vector expressed in LLF be defined as $\boldsymbol{x}_i$, then the two vectors are related as

$$\boldsymbol{x}_i = \boldsymbol{R}\, \boldsymbol{b}_i \tag{3}$$

where $\boldsymbol{R}$ is the attitude rotation matrix, $\boldsymbol{R} \in \mathbf{O}^{3\times 3}$, with $\mathbf{O}$ denoting the class of orthonormal matrices, that is $\boldsymbol{R}^T\boldsymbol{R} = \boldsymbol{I}_3$.

$\boldsymbol{R}$ can be described by a Direction Cosine Matrix (DCM) which is commonly used in many navigation applications. A three-dimensional rotation can be obtained by multiplying the three DCMs into a specific order, yielding the combined rotation matrix. Use of the

https://doi.org/10.1017/S0373463317000522 Published online by Cambridge University Press

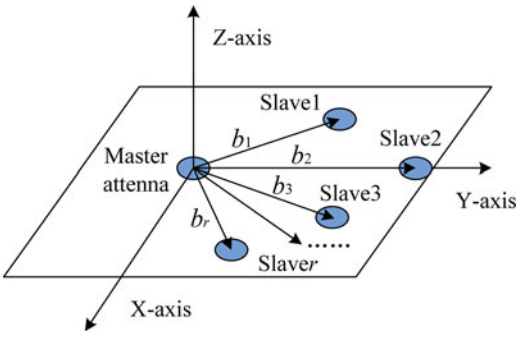


Figure 1. Baseline of GNSS antenna array in one platform.

yaw-pitch-roll sequence is given below

$$\boldsymbol{R} = \begin{bmatrix} \mathrm{c}_r\mathrm{c}_y - \mathrm{s}_r\mathrm{s}_p\mathrm{s}_y & \mathrm{c}_r\mathrm{s}_y + \mathrm{s}_r\mathrm{s}_p\mathrm{s}_y & -\mathrm{s}_r\mathrm{c}_p \\ -\mathrm{c}_p\mathrm{s}_y & \mathrm{c}_p\mathrm{c}_y & \mathrm{s}_y \\ \mathrm{s}_r\mathrm{c}_y + \mathrm{c}_r\mathrm{s}_p\mathrm{s}_y & \mathrm{s}_r\mathrm{s}_y - \mathrm{c}_r\mathrm{s}_p\mathrm{c}_y & \mathrm{c}_r\mathrm{c}_p \end{bmatrix} \tag{4}$$

where c and s denote the cosine and sine operators respectively. The y, p and r are shorthand notations for yaw, pitch and roll angles, respectively.

Let the baseline vector $\boldsymbol{b}_i$ be collected in the $3 \times r$ matrix $\boldsymbol{B} = \begin{bmatrix} \boldsymbol{b}_1 & \boldsymbol{b}_2 \ldots \boldsymbol{b}_r \end{bmatrix}$ and let the corresponding $\boldsymbol{x}_i$ be collected in the $3 \times r$ matrix $\boldsymbol{X} = \begin{bmatrix} \boldsymbol{x}_1 & \boldsymbol{x}_2 & \ldots & \boldsymbol{x}_r \end{bmatrix}$. Then the two matrices $\boldsymbol{X}$ and $\boldsymbol{B}$ are linked as

$$\boldsymbol{X} = \boldsymbol{RB}, \boldsymbol{X} \in \mathcal{R}^{3\times r}, \ \boldsymbol{B} \in \mathcal{R}^{3\times r}, \ \boldsymbol{R} \in \mathbf{O}^{3\times 3} \tag{5}$$

If the $r + 1$ GNSS antennae simultaneously track the same $s + 1$ GNSS satellites on the same f frequencies, and under the assumption of short baseline separations between antennae, the DD observation equations for the set of $2fsr$ code and carrier phase DD measurements can be formulated (Giorgi and Teunissen, 2013; Nadarajah, et al., 2013)

$$\mathrm{E}(\boldsymbol{Y}) = \boldsymbol{MX} + \boldsymbol{NZ}, \ \boldsymbol{Z} \in \boldsymbol{Z}^{fs\times r}, \ \boldsymbol{X} \in \mathcal{R}^{3\times r} \tag{6}$$

where $E(\cdot)$ represents the expectation operator, $\boldsymbol{Y}$ is the $2fs \times r$ matrix whose columns contain the DD code and phase observations from each baseline. $\boldsymbol{Z}$ is the $2fs \times r$ matrix of integer ambiguities. The $\boldsymbol{M}$ is the $2fs \times 3$ matrix of DD unit line-of-sight vectors and $\boldsymbol{N}$ is the $2fs \times fs$ matrix containing the carrier wavelengths.

The variance-covariance (v-c) matrix of observation matrix $\boldsymbol{Y}$ is given as

$$\mathrm{D}(\mathrm{vec}(\boldsymbol{Y})) = \boldsymbol{Q}_{YY} = \boldsymbol{P} \otimes \boldsymbol{Q}_{yy} \tag{7}$$

where vec(·) operator means stacking the columns of the $2fs \times r$ matrix $\boldsymbol{Y}$ into the vector vec($\boldsymbol{Y}$) of order $2fsr$. D(·) represents the dispersion operator so that the dispersion of vec($\boldsymbol{Y}$) is presented as v-c matrix $\boldsymbol{Q}_{YY}$. The $\boldsymbol{Q}_{yy}$ is $2fs \times 2fs$ v-c matrix that describes the dispersion of each set of baseline observations, and $\boldsymbol{P}$ is the $r \times r$ matrix that introduces correlation between baseline observations due to the common antenna used to form the DD observations.

https://doi.org/10.1017/S0373463317000522 Published online by Cambridge University Press

3. INTEGRATED ATTITUDE AND POSITION DETERMINATION WITH AFFINE CONSTRAINT.

3.1. *Attitude determination based on UC-AM.* The unconstrained attitude determination method does not make full use of the redundant information, such as the baseline length, the baseline orientation, the properties of the attitude matrix, the relationships between integer ambiguities and so on, which is referred to as the Unconstrained Attitude Model (UC-AM). Corresponding to UC-AM is the constraint model, according to the constraint strength and complexity, the OC-AM (Orthonormality Constrained) and AC-AM (Affine Constrained) model are proposed. The validity of integrated attitude and position determination based on OC-AM has been proved in a few references, such as Nadarajah et al. (2014a) and Buist (2013). However, the OC-AM has remarkable complexity, which is proven in Teunissen (2012) and Giorgi and Teunissen (2013). In these two references, the complexity and the accuracy of OC-AM, UC-AM and AC-AM are studied, and the theoretical and experimental results show that AC-AM can avoid the complexity of OC-AM, and still has better performance than UC-AM. In this paper, AC-AM is further applied to integrated attitude and position determination, and its advantage is compared to UC-AM.

Usually, the UC-AM first calculates the baseline matrix $\boldsymbol{X}$ based on Equation (6), then substitutes it in Equation (5) to calculate the attitude matrix $\boldsymbol{R}$. Two representative methods based on UC-AM, namely the direct attitude determination and the carrier smoothed pseudo-range methods are chosen (Dai et al., 2009). As shown in Figure 1, the coordinates of antennae 2 and 3 in the ABF can be expressed as $\boldsymbol{b}_2 = \begin{bmatrix} 0 & b_2 & 0 \end{bmatrix}^{\mathrm{T}}$ and $\boldsymbol{b}_3 = \begin{bmatrix} x_{3,b} & y_{3,b} & 0 \end{bmatrix}^{\mathrm{T}}$. Substituting $\boldsymbol{b}_2$ into Equation (3) and applying Equation (4) yields

$$\boldsymbol{x}_2 = \begin{bmatrix} x_{2,l} \\ y_{2,l} \\ z_{2,l} \end{bmatrix} = b_2 = \begin{bmatrix} -c_{\mathrm{p}} s_{\mathrm{y}} \\ c_{\mathrm{p}} c_{\mathrm{y}} \\ s_{\mathrm{p}} \end{bmatrix} \tag{8}$$

Then the yaw and pitch angles can be calculated directly as

$$y = -\tan^{-1}\left(\frac{x_{2,l}}{y_{2,l}}\right);\ p = \tan^{-1}\left(\frac{z_{2,l}}{\sqrt{x_{2,l}^2 + y_{2,l}^2}}\right) \tag{9}$$

The coordinate of antenna 3 is used to calculate the roll angle, as follows

$$\begin{bmatrix} x'_{3,l} \\ y'_{3,l} \\ z'_{3,l} \end{bmatrix} = R_p R_y = \begin{bmatrix} x_{3,l} \\ y_{3,l} \\ z_{3,l} \end{bmatrix} \Rightarrow r = -\tan^{-1}\left(\frac{z'_{3,l}}{x'_{3,l}}\right) \tag{10}$$

As can be seen from Equations (9) and (10), the direct attitude determination is relatively simple, but it does not employ the redundant measurements when more than three antennae are available. To make full use of all measurements, the carrier smoothed pseudo range approach can be used. Using the linearization of Equation (5) around the initial attitude y_0,

https://doi.org/10.1017/S0373463317000522 Published online by Cambridge University Press

r_0 and p_0, the attitude estimation model can be constructed as

$$\begin{bmatrix} \boldsymbol{A}_1 \\ \\ \boldsymbol{A}_2 \\ \cdots \\ \boldsymbol{A}_r \end{bmatrix} \begin{bmatrix} \Delta y \\ \Delta p \\ \Delta r \end{bmatrix} + \begin{bmatrix} |\boldsymbol{R}_0 - \boldsymbol{I}| & \boldsymbol{O} & \cdots & \boldsymbol{O} \\ \boldsymbol{O} & |\boldsymbol{R}_0 - \boldsymbol{I}| & \cdots & \boldsymbol{O} \\ \cdots & \cdots & \cdots & \cdots \\ \boldsymbol{O} & \boldsymbol{O} & \cdots & |\boldsymbol{R}_0 - \boldsymbol{I}| \end{bmatrix} \times \left(\begin{bmatrix} \boldsymbol{x}_1 \\ \boldsymbol{b}_1 \\ \boldsymbol{x}_2 \\ \boldsymbol{b}_2 \\ \cdots \\ \boldsymbol{x}_r \\ \boldsymbol{b}_r \end{bmatrix} - \begin{bmatrix} \Delta \boldsymbol{x}_1 \\ \Delta \boldsymbol{b}_1 \\ \Delta \boldsymbol{x}_2 \\ \Delta \boldsymbol{b}_2 \\ \Delta \ldots \\ \Delta \boldsymbol{x}_r \\ \Delta \boldsymbol{b}_r \end{bmatrix} \right) = 0 \tag{11}$$

where $\boldsymbol{R}_0$ is the rotation matrix at y_0, r_0 and p_0. $\Delta \boldsymbol{b}_i$ and $\Delta \boldsymbol{x}_i$ represent the errors of antenna r in the ABF and LLF coordinates. $\boldsymbol{I}$ is the identity matrix and $\boldsymbol{O}$ is the zero matrix. We represent the rotation matrix as a column vector $\boldsymbol{R} = \begin{bmatrix} r_1 & r_2 & r_3 \end{bmatrix}^{\mathrm{T}}$, then $\boldsymbol{A}_i$ is described as

$$\boldsymbol{A}_i = \begin{bmatrix} \dfrac{\partial(\boldsymbol{r}_1 \boldsymbol{x}_i)}{\partial y} & \dfrac{\partial(\boldsymbol{r}_1 \boldsymbol{x}_i)}{\partial p} & \dfrac{\partial(\boldsymbol{r}_1 \boldsymbol{x}_i)}{\partial r} \\ \dfrac{\partial(\boldsymbol{r}_2 \boldsymbol{x}_i)}{\partial y} & \dfrac{\partial(\boldsymbol{r}_2 \boldsymbol{x}_i)}{\partial p} & \dfrac{\partial(\boldsymbol{r}_2 \boldsymbol{x}_i)}{\partial r} \\ \dfrac{\partial(\boldsymbol{r}_3 \boldsymbol{x}_i)}{\partial y} & \dfrac{\partial(\boldsymbol{r}_3 \boldsymbol{x}_i)}{\partial p} & \dfrac{\partial(\boldsymbol{r}_3 \boldsymbol{x}_i)}{\partial r} \end{bmatrix} \tag{12}$$

Based on the least squares principle, the correction values for the attitude can be calculated as

$$\begin{bmatrix} \Delta y \\ \Delta p \\ \Delta r \end{bmatrix} = - \left[\sum_{i=2}^{n} \boldsymbol{A}_i^T \left(\boldsymbol{R}_0^T \boldsymbol{C}_{xi} \boldsymbol{R}_0 + \boldsymbol{C}_{bi} \right)^{-1} \boldsymbol{A}_i \right]^{-1} \times \left[\sum_{i=2}^{n} \boldsymbol{A}_i^T \left(\boldsymbol{R}_0^T \boldsymbol{C}_{xi} \boldsymbol{R}_0 + \boldsymbol{C}_{bi} \right)^{-1} \boldsymbol{W}_i \right] \tag{13}$$

where $\boldsymbol{C}_{xi}$ and $\boldsymbol{C}_{bi}$ represent the covariance matrices of $\boldsymbol{x}_i$ and $\boldsymbol{b}_i$, and $\boldsymbol{W}_i = \boldsymbol{R}_0 \boldsymbol{b}_i - \boldsymbol{x}_i$.

Then the correction value is iteratively used to update the attitude until the desired accuracy is achieved. This algorithm can use redundant measurements to improve the attitude accuracy. However, the baseline constraint information has still not been fully used.

3.2. *Attitude determination based on affine constraint.* Note that Equation (6) linearly relates the observation matrix $\boldsymbol{Y}$ to the unknown matrix parameters $\boldsymbol{X}$ and $\boldsymbol{Z}$ without considering the constraint information, thus Equation (6) is referred to as the UC-AM (Unconstrained Attitude Model). The above two methods are based on the UC-AM, which implies that Equation (3) or Equation (5) is only used after $\boldsymbol{X}$ has been solved using Equation (6), thus they will not benefit from the known geometry of the antenna array in the ABF.

If substituting Equation (5) into Equation (6), an alternative approach can be obtained, i.e. $\mathrm{E}(\boldsymbol{Y}) = \boldsymbol{MRB} + \boldsymbol{NZ}$, so that the relation of Equation (5) can be used from the beginning. Meanwhile, not all $3 \times r$ matrices $\boldsymbol{B}$ can be used to estimate a 3×3 matrix $\boldsymbol{R}$. For example, it is not possible to determine the rotation with configurations of r baselines obtained by lining up $r + 1$ antennae. Therefore, if the span of the baselines is not at the maximum, i.e.

https://doi.org/10.1017/S0373463317000522 Published online by Cambridge University Press

$q = \text{rank}(\boldsymbol{B}) < \min(3, r)$, the generalised relation can be expressed as

$$\mathrm{E}(\boldsymbol{Y}) = \boldsymbol{MRB} + \boldsymbol{NZ}, \quad \boldsymbol{Z} \in \mathrm{Z}^{fs\times r}, \quad \boldsymbol{R} \in \mathrm{O}^{3\times q} \tag{14a}$$

$$\mathrm{D}(\mathrm{vec}(\boldsymbol{Y})) = \boldsymbol{Q}_{YY} \tag{14b}$$

Equation (14) is called the OC-AM (Teunissen, 2007), in which the antenna geometry can be included from the beginning, because the orthonormal attitude matrix is $\boldsymbol{R} \in \mathrm{O}^{3\times q}$ instead of $\boldsymbol{X} \in \mathcal{R}^{3\times r}$ in the UC-AM. The orthonormality constraint results in a stronger model. However, this nonlinear constraint significantly increases the complexity of attitude computation and ambiguity resolution.

If one disregards the orthonormality constraint of the attitude matrix, a model of intermediate strength called the Affine Constrained Attitude Model (AC-AM) is obtained (Teunissen, 2012; Giorgi and Teunissen, 2013)

$$\mathrm{E}(\boldsymbol{Y}) = \boldsymbol{MRB} + \boldsymbol{NZ}, \quad \boldsymbol{Z} \in \mathrm{Z}^{fs\times r}, \quad \boldsymbol{R} \in \Re^{3\times q} \tag{15a}$$

$$\mathrm{D}(\mathrm{vec}(\boldsymbol{Y})) = \boldsymbol{Q}_{YY} \tag{15b}$$

As can be seen from Equations (15) and (14), the $\boldsymbol{R} \in \mathrm{O}^{3\times q}$ in OC-AM is replaced by the $\boldsymbol{R} \in \mathcal{R}^{3\times q}$ in AC-AM. The affine constraint implies the formulation of an affine transformation between body and reference-frame, which not only avoids the complexity of OC-AM, but also imposes a set of $r - q$ linear constraints if $r > q$. The AC-AM model can be solved by using the principles of multivariate integer least-squares solution (Teunissen, 2007; 2012), that is

$$\left[\breve{\boldsymbol{Z}}_{\mathrm{ac}} \quad \breve{\boldsymbol{R}}_{\mathrm{ac}}\right]^T = \arg \min_{\boldsymbol{Z}\in\mathcal{Z}^{fs\times r}, \boldsymbol{R}\in\mathcal{R}^{3\times q}} \|\mathrm{vec}\,(\boldsymbol{Y} - \boldsymbol{MRB} - \boldsymbol{NZ})\|^2_{\boldsymbol{P}\otimes\boldsymbol{Q}_{yy}} \tag{16}$$

To solve Equation (16), without considering the integer constraints $\boldsymbol{Z} \in \boldsymbol{Z}^{fs\times r}$ at first, the so-called float solution, i.e. $\hat{\boldsymbol{Z}}_{\mathrm{ac}}$ and $\hat{\boldsymbol{R}}_{\mathrm{ac}}$ can be obtained

$$\hat{\boldsymbol{R}}_{\mathrm{ac}} = \left[\bar{\boldsymbol{M}}^T\boldsymbol{Q}_{yy}^{-1}\bar{\boldsymbol{M}}\right]^{-1}\bar{\boldsymbol{M}}^T\boldsymbol{Q}_{yy}^{-1}\boldsymbol{Y}\boldsymbol{P}^{-1}\boldsymbol{B}^T\left[\boldsymbol{B}\boldsymbol{P}^{-1}\boldsymbol{B}^T\right]^{-1} \tag{17a}$$

$$\hat{\boldsymbol{Z}}_{\mathrm{ac}} = \left[\boldsymbol{N}^T\boldsymbol{Q}_{yy}^{-1}\boldsymbol{N}\right]^{-1}\boldsymbol{N}^T\boldsymbol{Q}_{yy}^{-1}\left[\boldsymbol{Y} - \boldsymbol{M}\hat{\boldsymbol{R}}_{\mathrm{ac}}\boldsymbol{B}\right] \tag{17b}$$

where $\bar{\boldsymbol{M}} = \left[\boldsymbol{I} - \boldsymbol{N}\boldsymbol{N}^-\right]\boldsymbol{M}$.

From the float solution, the fixed ambiguity solution can be formulated as

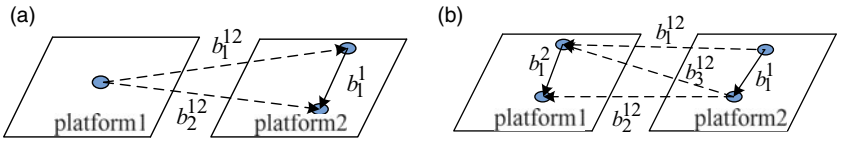
$$\breve{\boldsymbol{Z}}_{\mathrm{ac}} = \arg \min_{\boldsymbol{Z}\in\mathcal{Z}^{fs\times r}} \left\|\mathrm{vec}\left(\hat{\boldsymbol{Z}}_{\mathrm{ac}} - \boldsymbol{Z}\right)\right\|^2_{\boldsymbol{Q}_{\hat{Z}_{\mathrm{ac}}\hat{Z}_{\mathrm{ac}}}} \tag{18}$$

The ambiguity objective functions of $\breve{\boldsymbol{Z}}_{\mathrm{ac}}$ are quadratic forms in the entries of $\boldsymbol{Z}$, thus the minimisation problem can be solved by the standard LAMBDA method (Teunissen, 2003; Teunissen and Verhagen, 2011). Using the fixed $\boldsymbol{Z}$, the fixed solution $\breve{\boldsymbol{R}}_{\mathrm{ac}}(\boldsymbol{Z})$ can be further obtained

$$\breve{\boldsymbol{R}}_{\mathrm{ac}}(\boldsymbol{Z}) = \arg \min_{\boldsymbol{R}\in\mathcal{R}^{3\times q}} \left\|\mathrm{vec}\left(\hat{\boldsymbol{R}}_{\mathrm{ac}}(\boldsymbol{Z})\right) - \boldsymbol{R}\right\|^2_{\boldsymbol{Q}_{\hat{\boldsymbol{R}}_{\mathrm{ac}}(\boldsymbol{Z})\hat{\boldsymbol{R}}_{\mathrm{ac}}(\boldsymbol{Z})}} \tag{19}$$

Then the yaw y, pitch p and roll r can be obtained with the attitude matrix $\breve{\boldsymbol{R}}_{\mathrm{ac}}$.

https://doi.org/10.1017/S0373463317000522 Published online by Cambridge University Press



Three antennae configuration Four antennae configuration

Figure 2. The antenna configuration of double platforms.

Furthermore, if we let $\boldsymbol{N}^{-} = \left[\boldsymbol{N}^T\boldsymbol{Q}_{yy}^{-1}\boldsymbol{N}\right]^{-1}\boldsymbol{N}^T\boldsymbol{Q}_{yy}^{-1}$, the variance matrices of $\hat{\boldsymbol{Z}}_{\mathrm{ac}}$ and $\hat{\boldsymbol{R}}_{\mathrm{ac}}$ can be given as

$$\boldsymbol{Q}_{\hat{\boldsymbol{R}}_{\mathrm{ac}}\hat{\boldsymbol{R}}_{\mathrm{ac}}} = \left[\boldsymbol{B}\boldsymbol{P}^{-1}\boldsymbol{B}^T\right]^{-1} \otimes \left[\bar{\boldsymbol{M}}^T\boldsymbol{Q}_{yy}^{-1}\bar{\boldsymbol{M}}\right]^{-1} \tag{20a}$$

$$\boldsymbol{Q}_{\hat{\boldsymbol{Z}}_{\mathrm{ac}}\hat{\boldsymbol{R}}_{\mathrm{ac}}} = -\boldsymbol{B}^T\left[\boldsymbol{B}\boldsymbol{P}^{-1}\boldsymbol{B}^T\right]^{-1} \otimes \left[\boldsymbol{N}^{-1}\boldsymbol{M}\left[\bar{\boldsymbol{M}}^T\boldsymbol{Q}_{yy}^{-1}\bar{\boldsymbol{M}}\right]^{-1}\right] = \boldsymbol{Q}_{\hat{\boldsymbol{R}}_{\mathrm{ac}}\hat{\boldsymbol{Z}}_{\mathrm{ac}}}^T \tag{20b}$$

$$\boldsymbol{Q}_{\hat{\boldsymbol{Z}}_{\mathrm{ac}}\hat{\boldsymbol{Z}}_{\mathrm{ac}}} = \left[\boldsymbol{Q}_{\hat{\boldsymbol{Z}}_{\mathrm{uc}}\hat{\boldsymbol{Z}}_{\mathrm{uc}}}^{-1} + \boldsymbol{P}_{\mathrm{s}}\boldsymbol{P}^{-1} \otimes \boldsymbol{N}^T\boldsymbol{Q}_{yy}^{-1}\boldsymbol{M}\left[\boldsymbol{M}^T\boldsymbol{Q}_{yy}^{-1}\boldsymbol{M}\right]^{-1}\boldsymbol{M}^T\boldsymbol{Q}_{yy}^{-1}\boldsymbol{N}\right]^{-1} \tag{20c}$$

where $\boldsymbol{P}_{\mathrm{s}} = \boldsymbol{I} - \boldsymbol{P}^{-1}\boldsymbol{B}^T\left(\boldsymbol{B}\boldsymbol{P}^{-1}\boldsymbol{B}^T\right)^{-1}\boldsymbol{B}$. From Equation (20c) the inequality $\boldsymbol{Q}_{\hat{\boldsymbol{Z}}_{\mathrm{ac}}\hat{\boldsymbol{Z}}_{\mathrm{ac}}} < \boldsymbol{Q}_{\hat{\boldsymbol{Z}}_{\mathrm{uc}}\hat{\boldsymbol{Z}}_{\mathrm{uc}}}$ can be obtained (Giorgi and Teunissen, 2013), which means that the variance of $\hat{\boldsymbol{Z}}_{\mathrm{ac}}$ is smaller than the variance of $\hat{\boldsymbol{Z}}_{\mathrm{uc}}$. Thus, the affine constraint improves the precision of the ambiguity float solution, and this conclusion can also be proved by using the Ambiguity Dilution of Precision (ADOP) (Teunissen, 2012).

3.3. *Integrated attitude and position determination using AC-AM.* From the above discussion one can see that the ambiguity and attitude solution performance can be improved by using the AC-AM. Furthermore, the AC-AM can be shown to improve the performance of the integrated attitude and position determination system.

To analyse the mechanism of how to improve the relative positioning performance based on the AC-AM method, the method presented in Buist et al. (2009) is used, and the relatively simple configurations of three antennae and four antennae are discussed as shown in Figure 2. The solid line indicates a constrained baseline and the dotted line is an unconstrained baseline.

For the three antennae configuration in Figure 2(a), the baselines meet

$$\boldsymbol{b}_2^{12} = \boldsymbol{b}_1^1 + \boldsymbol{b}_1^{12}, \quad \boldsymbol{z}_2^{12} = \boldsymbol{z}_1^1 + \boldsymbol{z}_1^{12}, \quad \boldsymbol{y}_2^{12} = \boldsymbol{y}_1^1 + \boldsymbol{y}_1^{12}, \tag{21}$$

where $\boldsymbol{b}_1^1$ represents the constrained baseline vector, in which the superscript indicates the platform number and the subscript presents the indicator. $\boldsymbol{b}_1^{12}$ and $\boldsymbol{b}_2^{12}$ are the unconstrained baselines, in which the superscript indicates the relative baseline between platform 1 and platform 2 and the subscript presents the indicator.

$\boldsymbol{z}$ and $\boldsymbol{y}$ respectively represent the DD ambiguities and DD observation vectors corresponding to $\boldsymbol{b}$. Using the vector conversion relationship, the GNSS model can be

https://doi.org/10.1017/S0373463317000522 Published online by Cambridge University Press

established on a pair of arbitrary vectors, for example

$$\mathrm{E}\begin{bmatrix} \boldsymbol{y}_1^1 \\ \boldsymbol{y}_1^{12} \end{bmatrix} = \begin{bmatrix} \boldsymbol{A} & \boldsymbol{G} & 0 & 0 \\ 0 & 0 & \boldsymbol{A} & \boldsymbol{G} \end{bmatrix} \begin{bmatrix} \boldsymbol{z}_1^1 \\ \boldsymbol{b}_1^1 \\ \boldsymbol{z}_1^{12} \\ \boldsymbol{b}_1^{12} \end{bmatrix} \quad \mathrm{D}\begin{bmatrix} \boldsymbol{y}_1^1 \\ \boldsymbol{y}_1^{12} \end{bmatrix} = \begin{bmatrix} 1 & -\frac{1}{2} \\ -\frac{1}{2} & 1 \end{bmatrix} \otimes \boldsymbol{Q}_{yy} = \boldsymbol{P} \otimes \boldsymbol{Q}_{yy} \tag{22}$$

With the constraint on $\boldsymbol{b}_1^1$ and the corresponding ambiguities $\boldsymbol{z}_1^1$ of the single platform, which can be calculated by integer least-squares based on Equation (22), the optimal solution $\hat{\boldsymbol{b}}_1^{12}$ and the its v-c matrix with the baseline constraint can be obtained, that is

$$\hat{\boldsymbol{b}}_1^{12}\left(\boldsymbol{z}_1^{12}, \boldsymbol{b}_1^1\right) = \hat{\boldsymbol{b}}_1^{12}\left(\boldsymbol{z}_1^{12}\right) + \frac{1}{2}\left(\hat{\boldsymbol{b}}_1^1\left(\boldsymbol{z}_1^1\right) - \boldsymbol{b}_1^1\right) \tag{23a}$$

$$D\left(\hat{\boldsymbol{b}}_1^{12}\left(\boldsymbol{z}_1^{12}, \boldsymbol{b}_1^1\right)\right) = \frac{3}{4}\boldsymbol{Q}_{\hat{b}(z)\hat{b}(z)} \tag{23b}$$

Thus for the three antennae configuration, the constrained baseline accuracy can be improved from $\boldsymbol{Q}_{\hat{b}(z)\hat{b}(z)}$ to $3/4\boldsymbol{Q}_{\hat{b}(z)\hat{b}(z)}$. Similarly, for the four antennae configuration with two constrained baselines in Figure 2(b), the following relationships can be obtained

$$\hat{\boldsymbol{b}}_1^{12}\left(\boldsymbol{z}_1^{12}, \boldsymbol{b}_1^1, \boldsymbol{b}_1^2\right) = \hat{\boldsymbol{b}}_1^{12}\left(\boldsymbol{z}_1^{12}\right) + \frac{1}{2}\left(\hat{\boldsymbol{b}}_1^1\left(\boldsymbol{z}_1^1\right) - \boldsymbol{b}_1^1\right) + \frac{1}{2}\left(\hat{\boldsymbol{b}}_1^2\left(\boldsymbol{z}_1^2\right) - \boldsymbol{b}_1^2\right) \tag{24a}$$

$$D\left(\hat{\boldsymbol{b}}_1^{12}\left(\boldsymbol{z}_1^{12}, \boldsymbol{b}_1^1, \boldsymbol{b}_1^2\right)\right) = \frac{1}{2}\boldsymbol{Q}_{\hat{b}(z)\hat{b}(z)} \tag{24b}$$

So for the four antennae configuration in Figure 2(b), the baseline accuracy can be improved to $1/2\boldsymbol{Q}_{\hat{b}(z)\hat{b}(z)}$.

As can be seen from the above mechanism analysis, using the baseline constraint can not only improve the performance of attitude and ambiguity resolution for a single platform, but also improve the relative positioning for multiple platforms. Based on the AC-AM, a new integrated attitude and position determination approach is presented in Figure 3.

As shown in Figure 3, firstly, the attitude DD model and positioning DD model can be established by using code observation P and phase carrier observation Φ defined in Equation (1). Then the high-performance attitude results $\breve{\boldsymbol{R}}_1(\boldsymbol{Z}_1)$ and $\breve{\boldsymbol{R}}_2(\boldsymbol{Z}_2)$ of platform 1 and platform 2 can be calculated by the AC-AM, and the corresponding high performance ambiguity results $\breve{\boldsymbol{Z}}_1$ and $\breve{\boldsymbol{Z}}_2$ of each platform can also be obtained by the AC-AM. The relative ambiguity $\boldsymbol{Z}_{12}$ of the two platforms can be calculated by the positioning DD model. The above results are further substituted into the following equation

$$\breve{\boldsymbol{Z}} = \arg\left(\min_{\boldsymbol{Z}\in Z^n}\left(\left\|\begin{matrix} vec\left(\hat{\boldsymbol{Z}}_1 - \boldsymbol{Z}_1\right) \\ vec\left(\hat{\boldsymbol{Z}}_2 - \boldsymbol{Z}_2\right) \\ \hat{\boldsymbol{Z}}_{12} - \boldsymbol{Z}_{12} \end{matrix}\right\|_{\boldsymbol{Q}_{\hat{z}\hat{z}}}^2 + \left\|\begin{matrix} vec\left(\hat{\boldsymbol{Z}}_1(\boldsymbol{Z}_1) - \boldsymbol{R}_1\right) \\ vec\left(\hat{\boldsymbol{Z}}_2(\boldsymbol{Z}_2) - \boldsymbol{R}_2\right) \\ \hat{\boldsymbol{b}}_{12}(\boldsymbol{Z}) - \boldsymbol{b}_{12} \end{matrix}\right\|_{\boldsymbol{Q}_{\hat{R}(Z)\hat{R}(Z)}}^2\right)\right) \tag{25}$$

where $\boldsymbol{Z} = \begin{bmatrix} \boldsymbol{Z}_1 & \boldsymbol{Z}_2 & \boldsymbol{Z}_{12} \end{bmatrix}$ is the full matrix of ambiguities, and $\breve{\boldsymbol{Z}}$ is the final optimal result of $\boldsymbol{Z}$. $\boldsymbol{R} = \begin{bmatrix} \boldsymbol{R}_1 & \boldsymbol{R}_2 & \boldsymbol{b}_{12} \end{bmatrix}$ represents the full matrix of unknowns, in which $\boldsymbol{b}_{12}$ is relative baseline of two platforms. To solve Equation (25), the combining between-platforms

https://doi.org/10.1017/S0373463317000522 Published online by Cambridge University Press

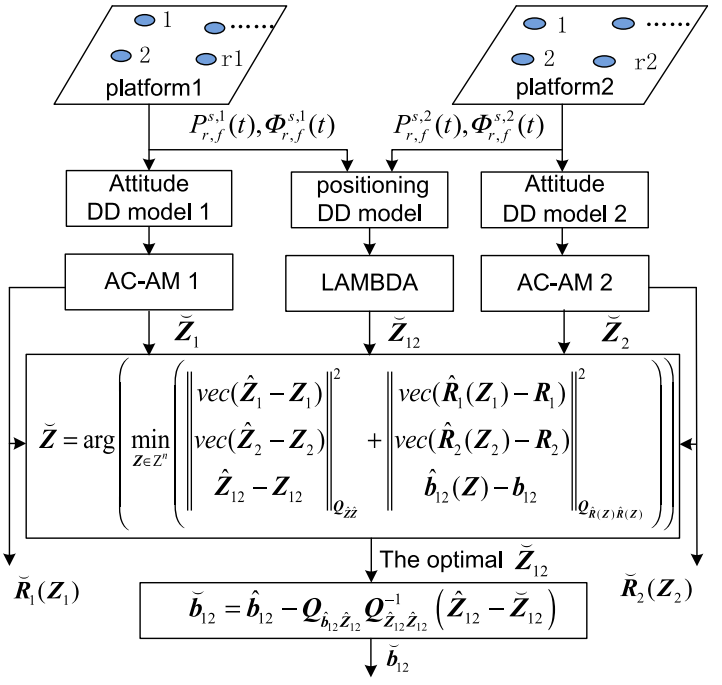


Figure 3. The schematic of integrated attitude and position determination using AC-AM.

equation can be established, and the attitude bootstrapping method is used (Buist et al., 2013; Nadarajah et al., 2014a). After the optimal $\breve{Z}_{12}$ is obtained, the relative baseline, i.e. the relative position can be further calculated, that is

$$\breve{b}_{12} = \hat{b}_{12} - Q_{\hat{b}_{12}\hat{Z}_{12}} Q^{-1}_{\hat{Z}_{12}\hat{Z}_{12}} \left(\hat{Z}_{12} - \breve{Z}_{12} \right) \tag{26}$$

Both the proposed method based on AC-AM and the method using OC-AM described in Nadarajah et al. (2014a) and Buist et al. (2009), can use the constrained information available, i.e. the integer property of the ambiguities, the relationship between the ambiguities on different baselines, and the known baseline length to determine the attitude and position of a multi-antenna system, thus significantly improving the success rate and accuracy of the solution compared with the UC-AM method. The difference is that the OC-AM uses MC-LAMBDA for ambiguity resolution, which significantly increases complexity and requires higher computational load. In contrast the AC-AM ignores the orthonormality so that the standard LAMBDA can be used, and it has lower computational complexity than the OC-AM and guarantees higher performance than the UC-AM.

Therefore, in this paper the standard LAMBDA algorithm is applied to solve the AC-AM model. A four-step procedure is employed in in the LAMBDA algorithm (Teunissen, 2003; Teunissen and Verhagen, 2011). In the integer estimation step, Integer Least-Squares (ILS) is selected as the mapping function, and the search with shrinking technique is used. In the acceptance test step, the Ratio Test is used for ambiguity validation. The bootstrapped-based lower bound P_{LB} is used to evaluate the ambiguity success rates, that

https://doi.org/10.1017/S0373463317000522 Published online by Cambridge University Press

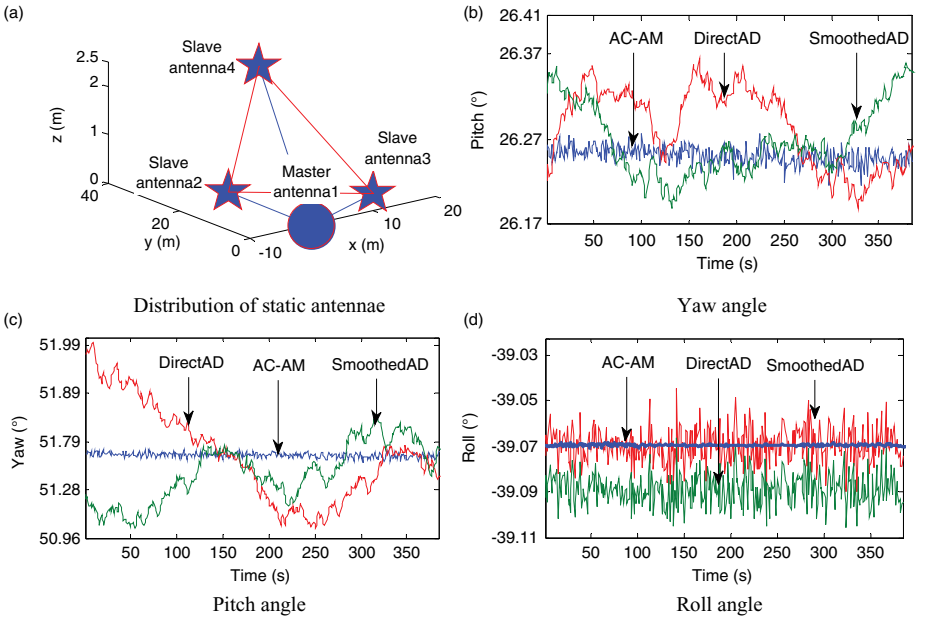


Figure 4. Distribution of static antennae and results of attitude determination.

is given as (Teunissen and Verhagen, 2011; Giorgi and Teunissen, 2013)

$$P_{\mathrm{LB}} = \prod_{i=1}^{n} 2\Phi\left(\frac{1}{2\sigma_{i|I}} - 1\right) \tag{27}$$

with $\Phi(x)$ representing the cumulative normal distribution and $\sigma_{i|I}$ is the sequential conditional variance of the ith ambiguity (conditioned on the previous $I = 1, \ldots, i-1$ ambiguities).

4. EXPERIMENTAL RESULTS AND ANALYSIS.

4.1. *Static data analysis.* To validate the AC-AM method, static and dynamic tests are carried out. For the static test, the data sets in Dai et al. (2009) are used, in which Global Positioning System (GPS) measurements are produced by a NovAtel® DL-4 receiver and IFEN NavX® FR GPS simulator, and the observation data rate is 1 Hz. The location of four static antennae, i.e. one master antenna and three slave antennae are accurately determined, as shown in Figure 4(a). The coordinate and attitude information of the antennae have been precisely determined in advance, and the yaw, pitch and roll angle are 51·666°, 26·182° and −39·073° respectively. The two UC-AM methods, i.e. DirectAD and SmoothedAD, which are the abbreviations of the direct attitude determination and the carrier smoothed pseudorange attitude determination described in Section 3.1, compared with the new proposed AC-AM method were used for attitude determination. The compared results are shown in Figure 4 and Table 1. As can be seen, the difference is not obvious between DirectAD and SmoothedAD, however, the performance of the AC-AM method is much better than the two traditional methods. In the static test, the four antennae are mainly used to validate

https://doi.org/10.1017/S0373463317000522 Published online by Cambridge University Press

Table 1. Results of attitude determination using static data.

Method		DirectAD	SmoothedAD	AC-AM
Mean	Yaw (°)	51·776	51·737	51·772
	Pitch (°)	26·284	26·273	26·256
	Roll (°)	−39·085	−39·095	−39·088
Std	Yaw (°)	0·084	0·060	0·005
	Pitch (°)	0·043	0·043	0·009
	Roll (°)	0·008	0·007	0·001
Success rate of ambiguity resolution	%	64	64	100

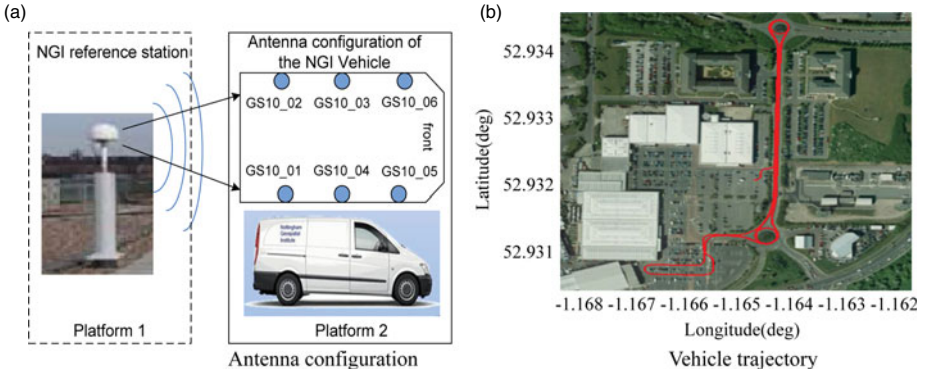


Figure 5. The dynamic test scenario in NGI.

the AC-AM model for attitude, and the relative position is not considered. The positioning performance will be further verified in a dynamic test.

4.2. *Dynamic test and analysis.* The dynamic experiment was carried out in the Nottingham Geospatial Institute (NGI) of the University of Nottingham. Six Leica GS10 GPS receiver antennae were mounted on the roof of a road vehicle, which is assumed to be platform 2, and the GPS reference station is assumed to be platform 1, as shown in Figure 5(a). The GPS observation data rate is 10 Hz, and the trajectory of vehicle is shown in Figure 5(b). The Inertial Navigation System (INS) (Applanix POS/RS with Honeywell C-IMU) and Leica Nova TS50 are integrated to provide a reference attitude and position solution. The coordinate matrix of the six antennae (GS10_01 ∼ 06) is

$$\boldsymbol{B} = \begin{bmatrix} 0.307 & -1.038 & -1.000 & 0.314 & 0.328 & -1.025 \\ -0.626 & -0.616 & 0.961 & 0.954 & 2.537 & 2.542 \\ 0.543 & 0.549 & 0.563 & 0.561 & 0.583 & 0.583 \end{bmatrix} \tag{28}$$

Firstly, the new AC-AM and UC-AM are compared with the success rate of ambiguity resolution. Three groups of antenna combination, i.e. 01-02-03-04, 01-02-03-04-05 and 01-02-03-04-05-06 are selected. In case of single frequency and single epoch, the success rates with five to ten visible satellites are shown in Figure 6. As can be seen, the performance of AC-AM is significantly better than UC-AM, especially in the situation of more antennae and fewer visible satellites, as shown in Figure 6(c). In addition, the success rate of UC-AM increases with the number of visible satellites rather than antenna configuration. However,

https://doi.org/10.1017/S0373463317000522 Published online by Cambridge University Press

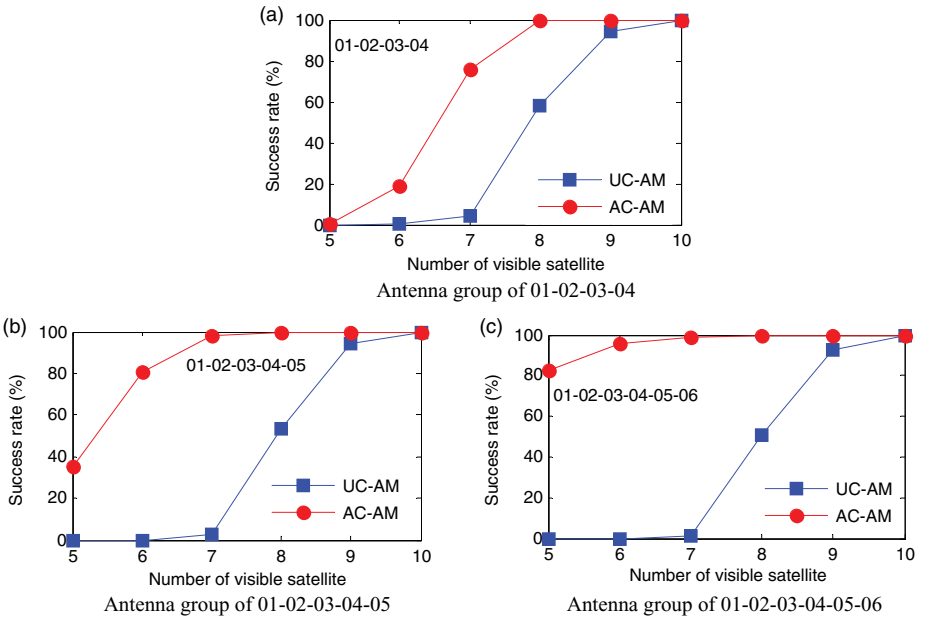


Figure 6. The success rate of ambiguity resolution for attitude determination using AC-AM vs. UC-AM.

Table 2. Results of attitude and position using dynamic data.

Method		DirectAD	SmoothedAD	AC-AM
Std of attitude error	Yaw (°)	1·574	1·465	0·262
	Pitch (°)	1·135	0·928	0·197
	Roll (°)	1·263	1·129	0·256
Std of position error	Baseline(m)		0·033	0·008
Success rate of ambiguity resolution	%		67	99

the success rate of AC-AM increases significantly with both the number of satellites and antennae.

Secondly, the attitude and relative position, namely the baseline results using the AC-AM and UC-AM methods are compared. To analyse the performance during vehicle manoeuvres, a period of data with a "dumbbell" movement (as shown in Figure 5(b)) is selected, and the attitude change calculated by INS is shown in Figure 7(a). The attitude and baseline results using an antenna group of 01-02-03-05 are shown in Figure 7 and Table 2.

As can be seen, these three methods reflect the trend of the attitude change of vehicle manoeuvre, which can be compared with the INS output. The SmoothedAD is slightly better than DirectAD, because it has the advantage of using redundant antennae for least square processing. Figure 7(e) shows the baseline results using UC-AM and AC-AM, which show no difference, maybe because the errors of the two methods are very small compared with the actual baseline changes. The difference of the two methods can be clearly shown using baseline error in Figure 7(f). The attitude and baseline results of AC-AM are the

https://doi.org/10.1017/S0373463317000522 Published online by Cambridge University Press

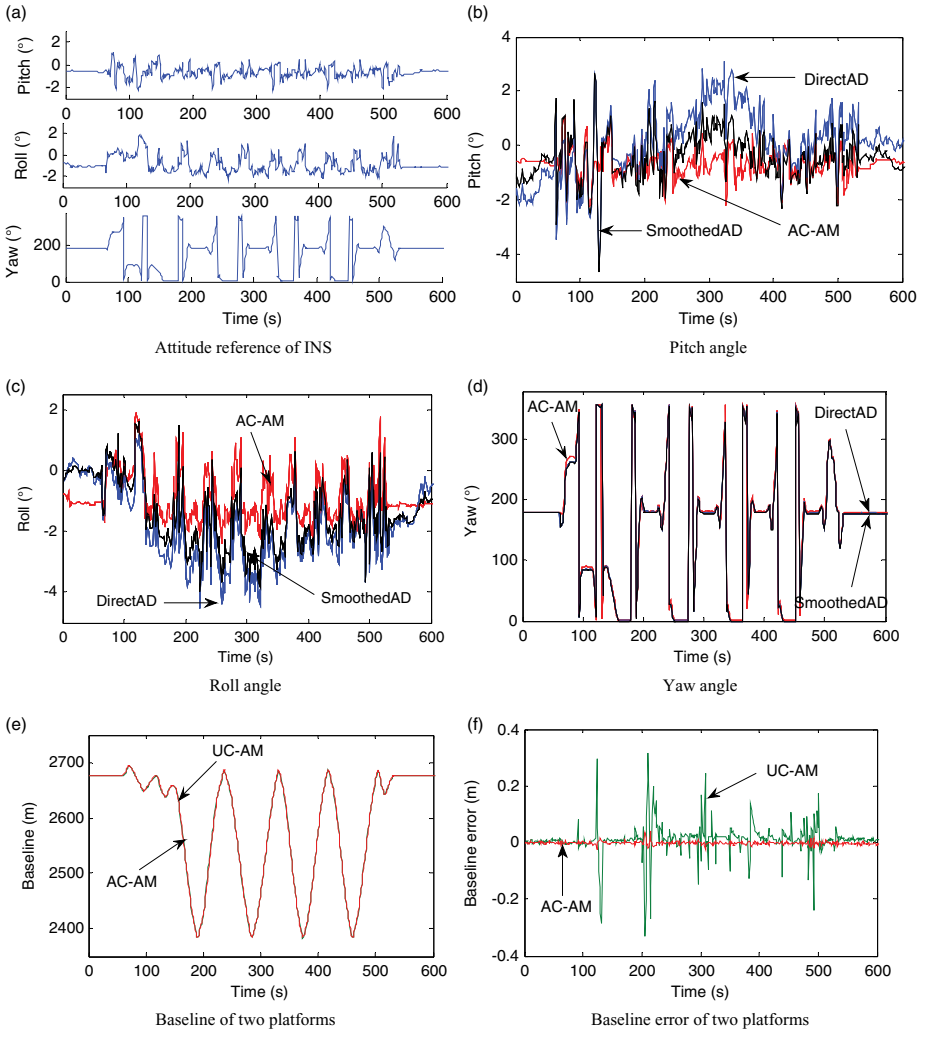


Figure 7. Attitude and position of vehicle manoeuvre using an antenna group of 01-02-03-05.

more consistent with the INS reference compared with the UC-AM method because more constraint information is used.

Lastly, a period of data with slow change is further analysed, and the attitude results of an antenna group of 01-02-05-06 are shown in Figure 8. It can be seen that the difference between the three methods is more obvious, in that the accuracy and stability using AC-AM have a significant improvement. The relative position errors between the vehicle and the reference station are presented in Figure 9. The antenna pairs of GS10_01, GS10_03 and GS10_05 from six antennae are randomly selected. As can be seen from all three cases, the position errors using the Affine Constraint are significantly smaller than the results using Unconstrained, which show the advantage of the proposed integrated method in this paper.

https://doi.org/10.1017/S0373463317000522 Published online by Cambridge University Press

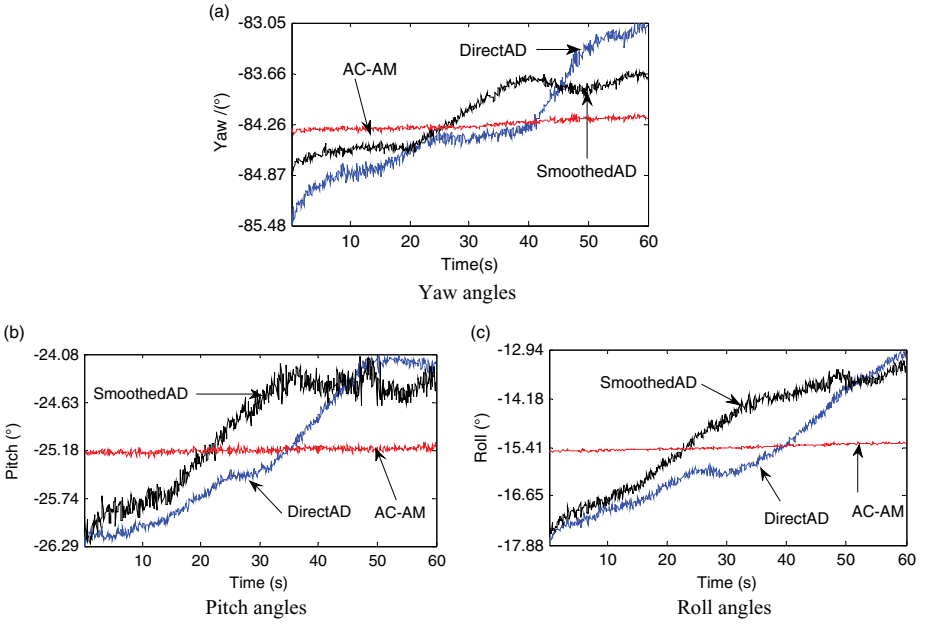


Figure 8. Attitude results of slow change using antenna groups of 01-02-05-06.

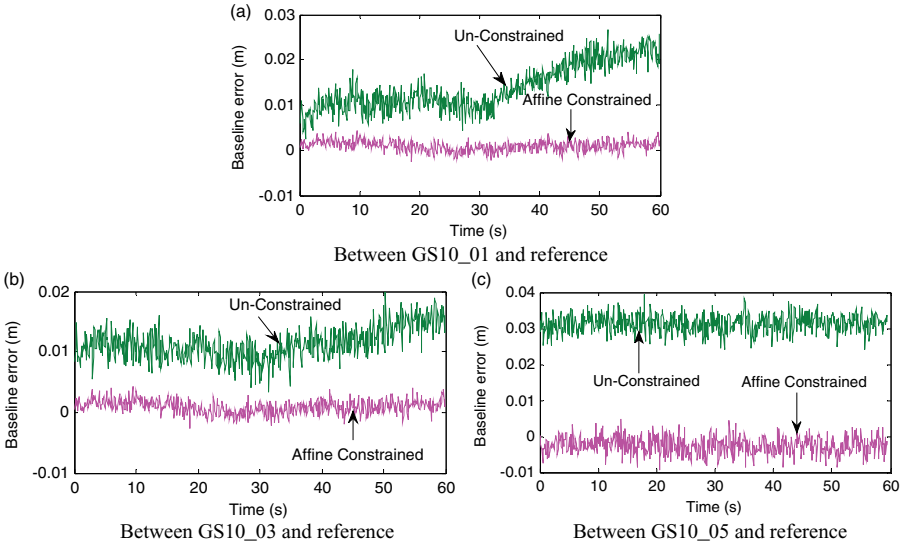


Figure 9. The baseline error of double platforms.

5. CONCLUSION. Currently, the two GNSS problems, attitude determination and positioning, are usually treated separately. This approach wastes some of the prior constrained information and neglects the internal connection between positioning and attitude determination, thus limiting the performance of ambiguity resolution and attitude and position output. This paper presents a new integrated attitude and position determination method

https://doi.org/10.1017/S0373463317000522 Published online by Cambridge University Press

based on an affine constraint. A series of actual static data and dynamic data from a GNSS experiment are obtained to demonstrate the new approach. Because more constraints are considered, the success rate of ambiguity resolution, the attitude, and the relative position outputs are obviously improved. This research provides a reference for the further study of an integrated GNSS positioning and attitude determination system.

ACKNOWLEDGMENT

Research for this paper was supported by the Natural Science of Jiangsu Province (KB20161490), Aviation Science Foundation of China (20150852013) and the Central Universities NUAA Fundamental Research Project (NS2015087). China Scholarship Council is gratefully acknowledged for supporting the first author's visiting periods at University of Nottingham. The authors also gratefully acknowledge the helpful comments and suggestions of the reviewers, which have improved the paper.

REFERENCES

Ardaens, J.S. and Florio, S.D. (2013). Autonomous formation flying based on GPS-PRISMA flight results. *Acta Astronautica,* **82**(1), 69–79.

Baroni, L. and Kuga, H.K. (2012). Analysis of attitude determination methods using GPS carrier phase measurements. *Mathematical Problem in Engineering*, 2012(1), 95–102.

Buist, P.J. (2013). *Multi-platform integrated positioning and attitude determination using GNSS*. Dissertation, Delft University of Technology.

Buist, P.J., Teunissen, P.J.G., Giorgi, G. and Verhagen, S. (2009). Multiplatform instantaneous GNSS ambiguity resolution for triple- and quadruple-antenna configurations with constraints. *International Journal of Navigation and Observation*, 2009, 1–14.

Dai, Z., Knedlik, S. and Loffeld, O. (2009). A MATLAB toolbox for attitude determination with GPS multi-antenna systems. *GPS Solutions*, **13**(3), 241–248.

Giorgi, G. and Teunissen, P.J.G. (2013). Low-complexity instantaneous ambiguity resolution with the affine-constrained GNSS attitude model. *IEEE Transactions on Aerospace and Electronic Systems*, **49**(3), 1745–1759.

Giorgi, G., Verhagen, S., Buist, P.J., and Teunissen, P.J.G. (2011a). GNSS based attitude determination: aerospace and formation flying. *Inside GNSS*, **6**(4), 62–71

Giorgi, G., Teunissen, P.J.G., Verhagen, S. and Buist, P.J. (2011b). Instantaneous ambiguity resolution in GNSS-based attitude determination applications: the MC-LAMBDA method. *Journal of Guidance, Control and Dynamics*, **35**(1), 51–67.

Hofmann, W.B., Lichtenegger, H. and Wasle, E. (2008). *GNSS-global navigation satellite systems*. Springer-Verlag, Wien, New York.

Jazaeri, S., Amiri-Simkooei, A. and Sharifi, M.A. (2014). On lattice reduction algorithms for solving weighted integer least squares problems: comparative study. *GPS Solutions*, **18**(1), 105–114.

Boeer, J., Steinbrecher, U., Bachmann, M., Schulze, D. and Braeutigam, B. (2014). Overview and status of TerraSAR-X /TanDEM-X long term system monitoring[C], *Proceedings of 10th European Conference on Synthetic Aperture Radar,* Berlin, Germany, 2014, 1–4

Lee, J.H., Sevil, H.E., Dogan, A. and Hullender, D. (2014). Estimation of receiver aircraft states and wind vectors in aerial refuelling. *Journal of Guidance, Control, and Dynamics*, **37**(1), 265–276.

Lenstra, A.K., Lenstra, H.W., Lova'sz, L. (1982). Factoring polynomials with rational coefficients. *Mathematische Annalen*, **261**(4), 513–534.

Li, B., Cao, H.J., Xu, J.N. and Zhu, Y. (2013). Application of carrier phase differential relative navigation for shipboard landing of aircraft. *China Satellite Navigation Conference (CSNC) Proceedings Lecture Notes in Electrical Engineering*, Vol. 243, 189–196.

Nadarajah, N., Paffenholz, J. and Teunissen, P.J.G. (2014a). Integrated GNSS Attitude Determination and Positioning for Direct Geo-Referencing. *Sensors,* **14**(7), 12715–12734.

Nadarajah, N., Teunissen, P.J.G. and Giorgi, G. (2014b). GNSS attitude determination for remote sensing: on the bounding of the multivariate ambiguity objective function. *Earth on the Edge: Science for a Sustainable Planet*, **139**, 503–509.

https://doi.org/10.1017/S0373463317000522 Published online by Cambridge University Press

Nadarajah, N., Teunissen, P.J.G. and Raziq, N. (2013). Instantaneous GPS–Galileo attitude determination: single-frequency performance in satellite-deprived environments. *IEEE Transactions on Vehicular Technology,* **62**(7), 2963–2976.

Seysen, M. (1993). Simultaneous reduction of a lattice basis and its reciprocal basis. *Combinatorica*, **13**(3), 363–376.

Stephenson, S., Meng, X. and Moore, T. (2014). Not just a fairy tale: a Hansel and Gretel approach to cooperative vehicle positioning. *GPS World*, **25**(7), 44–50.

Teunissen, P.J.G. (2003). Towards a unified theory of GNSS ambiguity resolutions. *Journal of Global Positioning System,***2**(1), 1–12.

Teunissen, P.J.G. (2007). A general multivariate formulation of the multi-antenna GNSS attitude determination problem. *Artificial Satellites,* **42**(2), 97–111.

Teunissen, P.J.G. (2012). The affine constrained GNSS attitude model and its multivariate integer least-squares solution. *Journal of Geodesy*, **86**(7), 547–563.

Teunissen, P.J.G. and Verhagen, S. (2011). Integer aperture estimation: a framework for GNSS ambiguity acceptance testing. *Inside GNSS*, **6**(2), 66–73

Werner, W. and Winkel, J. (2003). TCAR and MCAR options with Galileo and GPS. *Proceedings of the 16th International Technical Meeting of The Institute of Navigation*, Portland, OR, 790–800.

Yang, Y., Li, Y., Rizos, C., Dempster, A.G. and Yue, X. (2014). Inter-satellite ranging augmented GPS relative navigation for satellite formation flying. *The Journal of Navigation*, **67**(3), 437–449.

https://doi.org/10.1017/S0373463317000522 Published online by Cambridge University Press